BIOCHEMISTRY
including biophysical chemistry & molecular biology

ARTICLE

pubs.acs.org/biochemistry

Substrate-Dependent Conformational Dynamics of the *Escherichia coli* Membrane Insertase YidC

Nora Imhof,[‡] Andreas Kuhn,[‡] and Uwe Gerken*[,‡]

[‡]Institute of Microbiology, University of Hohenheim, Garbenstrasse 30, D-70599 Stuttgart, Germany

ABSTRACT: The binding of Pf3 coat protein to the membrane insertase YidC from *Escherichia coli* induces a conformational change in the tertiary structure of the insertase, resulting in a quenching of the intrinsic tryptophan (Trp) fluorescence. Tryptophan mutants of YidC were generated to examine such conformational movements in detail with time-resolved and steady-state fluorescence spectroscopy. Ten of the 11 Trp residues within YidC were substituted to phenylalanines generating single Trp mutants either at position 354, 454, or 508. In addition, a double mutant with Trp residues at 332 and 334 was studied. Purified YidC mutants were reconstituted into DOPC/DOPG vesicles and titrated with a Trp-free mutant of Pf3 coat, enabling a detailed conformational study of the periplasmic P1, P2, and P3 domains of YidC before and after binding of substrate. Time-resolved fluorescence anisotropy revealed that the mobility of the residues W332/W334 and W508 was considerably increased after binding of Pf3 coat to the insertase. Furthermore, analysis of the fluorescence emission spectra and the decay times showed that all Trp residues are embedded in an equivalent environment that is a membrane/water interface.

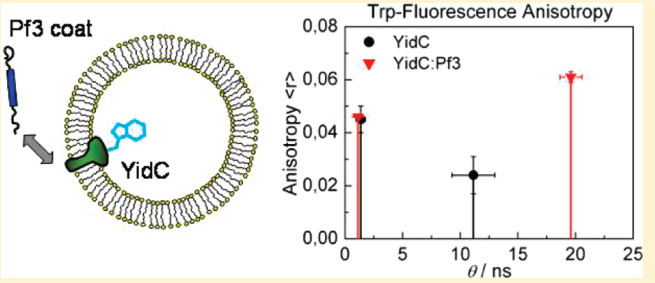

During membrane biogenesis the newly synthesized membrane proteins are inserted into the membrane by translocases and insertases. The most prominent system that exists in prokaryotes and in the endoplasmic reticulum of eukaryotes is the Sec translocase.[1] The Sec translocase spans the cytoplasmic membrane multiple times and forms a protein conducting channel that allows the translocation of a protein chain across the bilayer.[2] The translocase can also open the protein conducting channel laterally to release a membrane protein inserting it into the lipid bilayer.[3] By a coordinated interplay of both mechanisms, membrane proteins with large hydrophilic domains are simultaneously translocated and inserted into the cytoplasmic membrane.

Membrane proteins with small periplasmic domains use the interaction with YidC for insertion into the lipid bilayer.[4] Apart from the well-characterized coat proteins of filamentous phages M13 and Pf3,[5] ATPase subunit c[6] and the MscL protein of the mechanosensitive channel have been characterized as members of this YidC-only pathway.[7] YidC of *Escherichia coli* is a 61 kDa large, six-spanning membrane protein with a proposed topology as shown in Figure 1A.[8] The structure of the large periplasmic domain (P1) located between TM1 and TM2 has recently been solved by X-ray crystallography[9,10] and is displayed in Figure 1B.

When the YidC protein was purified and reconstituted into proteoliposomes, it was catalytically active and able to promote the insertion of Pf3 coat.[11] The purified reconstituted system allows the individual steps of membrane insertion to be investigated. We have previously shown, using steady-state fluorescence spectroscopy, that the binding of Pf3 coat to YidC is reversible and has a dissociation constant (K_D) of about 1 μM.[12] The binding process of the substrate Pf3 coat protein also was followed by quenching of the intrinsic Trp fluorescence of the insertase which indicates a substrate-induced conformational change of YidC.[13]

In the present work, we analyzed the binding process of membrane-reconstituted Trp mutants of YidC to Pf3 coat protein with time-resolved fluorescence as well as steady-state fluorescence spectroscopy in more detail. Individual Trp residues were located in each of the three periplasmic loop regions at positions 332/334, 354, 454, and 508, as shown in Figure 1A. We show that the conformational change induced by the binding process involves all periplasmic domains of YidC. In particular, the local surroundings of Trp residues at positions 332/334 and at 508 undergo large conformational events after Pf3 coat binding, resulting in an increased mobility of these residues. These results show that the substrate binding of Pf3 coat protein induces specific conformational changes in the periplasmic part of YidC. We also show that the surrounding of the residues W332/W334 (P1 loop) is equivalent to the environment of the other residues located at the perplasmic membrane/water interface of YidC.

MATERIALS AND METHODS

Generation, Expression, and Purification of YidC Trp Mutants. Wild-type *yidC* (with a C-terminal His_{10} tag) was

Received: December 21, 2010
Revised: February 25, 2011
Published: March 14, 2011

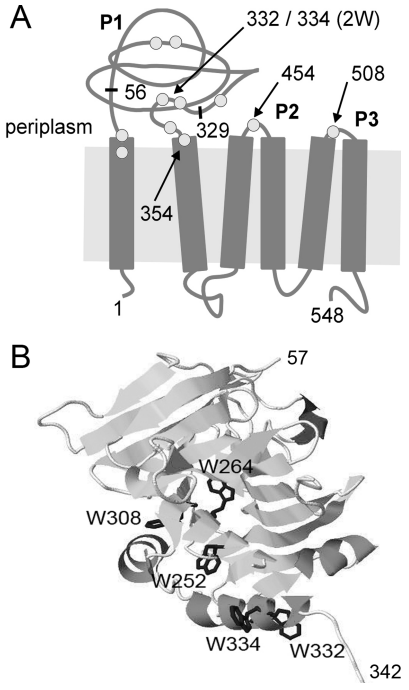

Figure 1. (A) Membrane topology of YidC with its periplasmic domains P1, P2, and P3. The numbers in the P1 domain indicate the positions of the amino acid residues flanking the segment of P1 which has been investigated as a separate fragment (56−329) in this study. The approximate positions of the 11 natural Trp residues along the structure are marked by gray circles and the arrows highlight the Trp residues left in the Trp mutants $YidC_{2W}$, $YidC_{W354}$, $YidC_{W454}$, and $YidC_{W508}$. (B) Structural representation of the periplasmic domain P1 (PDB ID: 3BLC[9]) showing the positions of the Trp residues.

cloned into pUC19.[14] This construct was used to create the single Trp mutants $YidC_{W354}$, $YidC_{W454}$, and $YidC_{W508}$ and the double tryptophan mutant $YidC_{W332/W334}$ (designated $YidC_{2W}$) via site-directed mutagenesis.[15] Thus, all Trp residues were substituted for Phe with the exception of the residues indicated in the subscripts.

The genes encoding the different *E. coli* YidC Trp mutants were each cloned into the expression vector pGZ119EH.[16] These plasmids were transformed into the *E. coli* strain C43(DE3). Cells were grown under aerobic conditions in Luria−Bertani (LB) medium at 37 °C. Protein expression was induced with 0.7 mM IPTG when an optical density ($OD_{605\ nm}$) of 0.5 was reached and continued for 16 h at 15 °C. Cells were harvested by centrifugation at 5000*g* for 10 min and resuspended in 1 mL of 2-amino-2-(hydroxymethyl)-1,3-propanediol (Tris) buffered saline (TBS) per gram of cells. Cells were broken by two passes in a French pressure cell at 8000 psi after the addition of a protease inhibitor cocktail (EDTA-free complete, Roche Diagnoststics GmbH). The cell debris was removed from the crude lysate by centrifugation at 5000*g* for 15 min and 4 °C, and the membrane fraction was collected by centrifugation at 220000*g* for 50 min and 4 °C. The membrane-containing pellet was solubilized for 1.5 h on ice in TBS buffer containing 1% (w/v) *n*-dodecyl-*β*-D-maltoside (DDM) (GERBU Biochemicals GmbH). The solubilized components were obtained by centrifugation at 240000*g* for 20 min and 4 °C. Subsequently, the supernatant was supplemented with 40 mM imidazole and then incubated with a Ni^{2+}-NTA matrix (Qiagen) for 1 h at 4 °C. The matrix was washed with TBS buffer supplemented with 60 mM imidazole and 0.03% (w/v) DDM, and the protein was eluted with TBS buffer containing 0.1% (w/v) DDM and 280 mM imidazole.

The homogeneity of the purified YidC and Pf3 coat proteins were tested with sodium dodecyl sulfate gel electrophoresis (SDS-PAGE), and the concentrations were determined using the Lowry−Peterson assay.[17]

Preparation of Phospholipids. 50 mg of a 1:1 (w/w) mixture of 1,2-dioleoyl-*sn*-glycero-3-phosphocholine (DOPC) and 1,2-dioleoyl-*sn*-glycero-3-phospho-(1′-*rac*-glycerol) (DOPG) (Avanti Polar Lipids, Inc.) were dissolved in 2 mL of $CHCl_3$ and dried for 6 h under vacuum as described.[13] The dried film was resuspended in 5 mL of H_2O, aerated with nitrogen, and stored at −80 °C. Unilamellar vesicles with a mean diameter of about 250 nm were obtained by extruding (Avanti Mini-Extruder, Avanti Polar Lipids, Inc.) the lipid emulsion 15 times through a membrane with a defined pore size (0.4 *μ*m, Whatman).

Membrane Reconstitution of YidC. The reconstitution followed the protocol described by Rigaud et al.[18] Prior to the reconstitution process, 12 mM DOPC/DOPG (1:1 w/w) phospholipid vesicles were incubated with 1.5 mM DDM for 3 days at 4 °C. For reconstitution, 1.5 mM of these liposomes was mixed with 3 *μ*M purified YidC protein and equilibrated for 2 h at 4 °C under gentle mixing. The detergent was removed within 3 h with 40 mg of BioBeads SM-2 (Bio-Rad Laboratories) at 4 °C. Proteoliposomes were sedimented by centrifugation for 10 min at 120000*g* and resuspended in 20 mM Tris-HCl buffer pH 7.0 containing 300 mM NaCl. The generated proteoliposomes had a diameter of about 150 nm.

Topology Analysis. Proteoliposomes (generated as described above) were resuspended in 100 *μ*L of 20 mM Tris-HCl pH 7.0 containing 200 mM NaCl. Trypsin (final concentration 0.05 mg/mL) was added, and proteolysis was conducted for 20 min at 25 °C. Subsequently, the sample was precipitated with trichloroacetic acid (TCA). A second sample of proteoliposomes was incubated without trypsin and likewise precipitated with TCA. Both samples were washed with acetone and analyzed by SDS-PAGE. Western blotting and immunolabeling with a primary antibody against the YidC P1 domain were carried out as described.[13] The ECL (Millipore Corp.) exposed film was quantified using the AIDA software package (Raytest, Germany). For a control, the DDM solubilized samples were digested and treated as described above.

Binding of Pf3W0 to DOPC/DOPG Liposomes. 15 mM DOPC/DOPG liposomes (1:1 w/w), prepared as described above, were incubated for 2 h with 21 *μ*M Pf3W0 in 20 mM Tris-HCl buffer pH 7.0 containing 300 mM NaCl and 5% (v/v) 2-propanol. Liposomes were sedimented by centrifugation for 10 min at 120000*g*. The supernatant was precipitated with TCA, and the pellet was resuspended in 20 mM Tris-HCl buffer pH 7.0 containing 300 mM NaCl and subsequently precipitated by TCA. Both samples were washed twice with acetone. Western blotting and immunolabeling with a primary antibody against Pf3 coat were carried out as described,[13] and the ECL (Millipore Corp.) exposed film was quantified using the AIDA software package (Raytest, Germany).

Expression and Purification of Wild-Type YidC and Domain P1. The YidC wild-type gene with a C-terminal His_{10} tag was cloned into the expression vector pMS119EH.[19] The plasmid was transformed into *E. coli* strain C43(DE3) and grown under aerobic conditions in LB medium at 37 °C until an $OD_{605\ nm}$ of 0.5 was reached. Protein expression with 0.7 mM

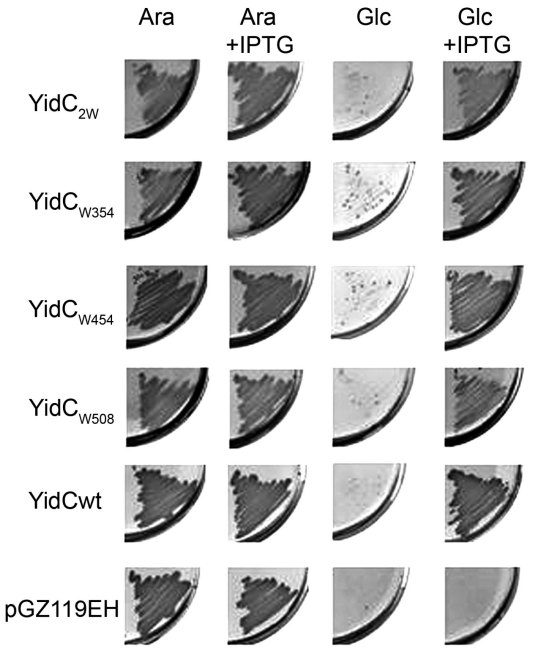

Figure 2. His-tagged YidC Trp mutants $YidC_{2W}$, $YidC_{W354}$, $YidC_{W454}$, and $YidC_{W508}$ as well as the His-tagged wild-type YidC complement the growth defect of YidC depletion strain *E. coli* JS7131. Cells containing the respective plasmid were grown on LB agar plates supplemented with arabinose (Ara) (chromosomal YidC expression), arabinose and IPTG (chromosomal YidC expression and expression of the plasmid encoded proteins), glucose (Glc) (chromosomal YidC repression), glucose and IPTG (chromosomal YidC repression and expression of the plasmid encoded protein), respectively. As a negative control the empty vector pGZ119EH was tested.

IPTG was allowed for 3 h at 37 °C. Cells were resuspended in TBS buffer and frozen at −80 °C. Purification was performed as for the full-length YidC as described above. The P1 domain including residues 56−329 of YidC was expressed and purified as previously described.[13]

Expression and Purification of Pf3W0 Coat Protein. The Trp-free mutant Pf3W0 coat was expressed from *E. coli* C41 bearing the plasmid pMS119HE containing the *pf3coat* gene and purified as described previously.[11]

Complementation Assay. The different YidC Trp mutants and the YidC wild-type (all with C-terminal His_{10} tags) were cloned into the vector pGZ119EH[16] under control of a *tac*-promoter. These constructs were transformed into the YidC depletion strain JS7131,[4] and overnight cultures grown in the presence of 0.2% arabinose were diluted 1:10 in LB medium. 5 μL of each culture was spotted on LB agar plates containing either arabinose and glucose (final concentration 0.2%), arabinose, and 1 mM IPTG or glucose and IPTG. The plates were incubated for 15 h at 37 °C. As negative control the empty vector pGZ119EH was treated likewise.

Steady-State Fluorescence Spectroscopy and Fluorometric Titration. All experiments were performed in a quartz microcuvette (Hellma AG) at a constant temperature of 25 °C using the same setup as previously described.[12] The Trp residues of the reconstituted YidC as well as of the P1 domain were excited at 295 nm, and the fluorescence was recorded between 305 and 450 nm with a step width of 1 nm and an integration time of 1 s. The slits of the excitation and emission monochromator were set to a spectral width of 2 and 3 nm, respectively. To test for tyrosine (Tyr) fluorescence, the sample was excited additionally at 290 and 280 nm.

Fluorescence spectra were measured in 20 mM Tris-HCl buffer pH 7.0 containing 300 mM NaCl and 5% (v/v) 2-propanol for the reconstituted YidC samples and wild-type YidC and in phosphate buffered saline (PBS) (pH 6.0) for the P1 domain.

Reconstituted YidC mutants were titrated with small aliquots of 27 μM Pf3W0 coat and allowed to equilibrate for 5 min. Subsequently, a fluorescence spectrum was recorded. All spectra were background-corrected by subtracting a buffer blank spectrum. The corrected spectra were analyzed by fitting to the log−normal distribution[20,21]

$$F(\lambda)_{\log\ -\ \mathrm{normal}} = F_0 \exp\left[-\frac{\ln 2}{\ln^2 \rho}\ln^2\left(1+\frac{(\lambda-\lambda_{\max})(\rho^2-1)}{\rho\Gamma}\right)\right] \quad (1)$$

where F_0 is the fluorescence maximum at λ_{max}, Γ is the full width at half-maximum (fwhm), and ρ determines the line-shape asymmetry. Binding curves were constructed from the recorded spectra by plotting $\Delta F_i = |F_i(1 + V_i/V_0) - F_0|$ against the molar Pf3W0 coat concentration [Pf3], where F_i is the maximum value of the fluoescence at the *i*th titration step and F_0 is the initial maximum value of the sample fluorescence without substrate. To compensate for the increasing volume due to titration, F_i has to be multiplied with $(1 + V_i/V_0)$, where V_i is the total added volume at the *i*th titration step and V_0 is the initial volume. The dissociation constant K_D for each mutant was then calculated by fitting the binding curve to the hyperbolic equation

$$\Delta F = \Delta F_{\max}\frac{[\mathrm{Pf3}]}{[\mathrm{Pf3}] + K_D} \quad (2)$$

where ΔF_{max} is the maximum fluorescence change at saturation. Data analysis was performed using Origin 6.1 software (OriginLab Corp.).

Fluorescence Decay and Time-Resolved Fluorescence Anisotropy Measurements. Time-resolved measurements were performed with a commercial fluorescence lifetime spectrometer (FluoTime 100, PicoQuant GmbH) equipped with a photomultiplier tube and a time correlated single photon counting (TCSPC) module (PicoHarp 300, PicoQuant GmbH) for the data acquisition. The sample was excited at 290 nm with a subnanosecond pulsed light-emitting diode (LED) (PLS 290, PicoQuant GmbH) at a repetition rate of 10 MHz (PDL 800-B, PicoQuant GmbH), and the sample holder was controlled by a bath thermostat (F3, Haake GmbH). Possible parasitic emission of the LED was blocked by a short-pass filter (FF01-310/SP-25, Semrock Inc.). The instrument response function (IRF) of this setup was measured with the stray light signal of a dilute colloidial silica suspension (Ludox) and had a fwhm of 700 ps, limited by the LED's pulse width. In order to block the Raman scattering band of the aqueous buffer, a suited bandpass filter with a center wavelength at 357 nm and a bandwidth of 44 nm (Brightline HC 357/44, AHF Analysentechnik AG) was installed in the fluorescence beam path.[22] To obtain vertical polarized LED pulses, a quartz polarizer (Linos Photonics AG) was introduced in the excitation beam path, and a thin film polarizer on a rotatable mount with a transmission wavelength range of 330−450 nm (Linos Photonics AG) was used to analyze the sample fluorescence.

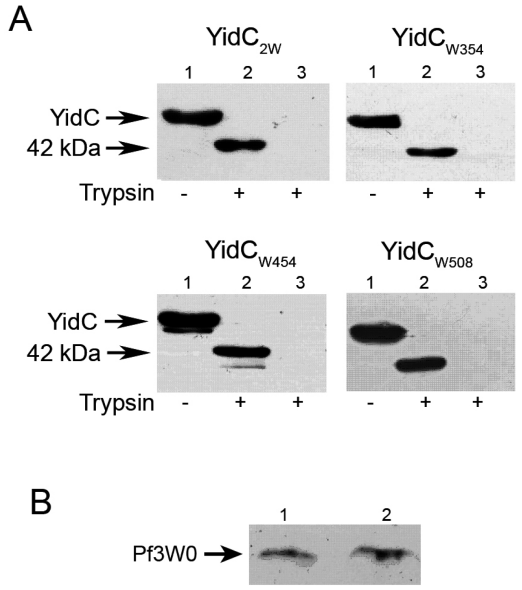

Figure 3. (A) Topological analysis of the reconstituted YidC mutants. Proteoliposomes were digested with trypsin. The undigested and digested samples are shown in lanes 1 and lanes 2, respectively. The full-length YidC and the 42 kDa fragment are denoted with an arrow. No fragments were detected after digestion of DDM solubilzed YidC mutants (lanes 3).The percentage of membrane reconstituted YidC with the P1 domain located in the lumen was determined with 65% for $YidC_{2W}$, 61% for $YidC_{W354}$, 66% for $YidC_{W454}$, and 69% for $YidC_{W508}$. (B) Binding of Pf3W0 coat to DOPC/DOPG liposomes. Pf3W0 coat was incubated with DOPC/DOPG liposomes and separated by ultracentrifugation. The supernatant and the pellet fraction are shown in lane 1 and lane 2, respectively. The Pf3W0 coat protein was found in both fractions in about equal amounts.

All fluorescence decay measurements were done at magic-angle conditions (emission polarizer set at 54.7°) with a time resolution of 64 ps/channel. The data were collected to a constant peak intensity of 1×10^4 counts. The lifetimes were recovered by fitting the fluorescence decays $I(t)$ to

$$I(t) = \int_{-\infty}^{t} \mathrm{IRF}(t') \sum_{i=1}^{n} I_0 \alpha_i \exp\left(-\frac{t-t'}{\tau_i}\right) \mathrm{d}t' \qquad (3)$$

where τ_i is the fluorescence lifetime and α_i indicates the fractional amplitudes of the ith lifetime component to the total amplitude I_0 ($\Sigma\alpha_i = 1$). The fractional contribution f_i of each lifetime component τ_i to the steady-state intensity is given by

$$f_i = \frac{\alpha_i \tau_i}{\sum_i \alpha_i \tau_i} \qquad (4)$$

Fluorescence anisotropy $r(t)$ of the reconstituted YidC mutants was calculated with

$$r(t) = \frac{I_{VV}(t) - G I_{VH}(t)}{I_{VV}(t) + 2G I_{VH}(t)} \qquad (5)$$

where $I_{VV}(t)$ and $I_{VH}(t)$ are the vertical and horizontal polarization components of the time-dependent fluorescence. The factor G accounts for the polarization-dependent sensitivity of the spectrometer and was 1.03 for our setup. Anisotropy measurements were done at a time resolution of 128 ps/channel, and data were collected to a peak intensity for the $I_{VV}(t)$ signal of at least

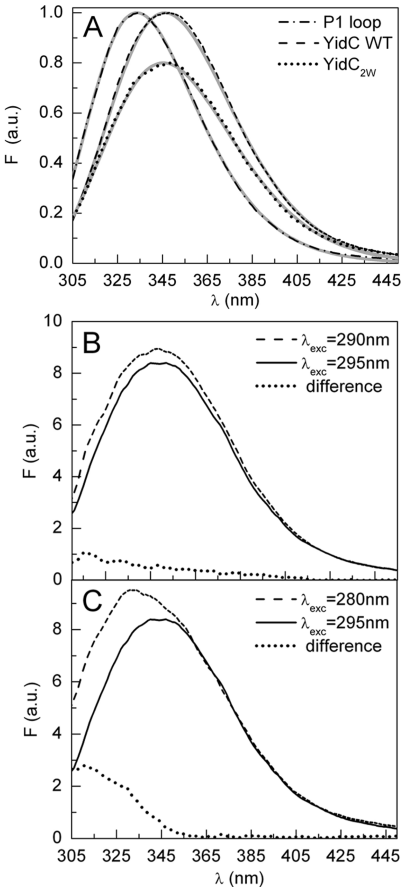

Figure 4. (A) Normalized intrinsic Trp fluorescence spectra of wild-type YidC, $YidC_{2W}$ (both reconstituted in DOPC/DOPG vesicles), and the P1 domain excited at 295 nm. For the reason for comparability the spectrum of $YidC_{2W}$ is displayed with lower intensity. The fitted log−normal curves (see eq 1) are overlaid (gray solid lines). Intrinsic Trp fluorescence spectra of reconstituted $YidC_{W508}$ excited at (B) 290 and 295 nm and (C) excited at 280 and 295 nm and the corresponding difference spectra. The fluorescence spectra are normalized to equal fluorescence yields at 420 nm [P1 domain in PBS (pH 6.0), YidC in 20 mM Tris-HCl (pH 7.0), and 300 mM NaCl and 5% (v/v) 2-propanol].

3×10^4 counts. The anisotropy data were analyzed by fitting to a double-exponential model

$$r(t) = r_\infty + \sum_{i=1}^{2} r_i \exp(-t/\theta_i) \qquad (6)$$

where r_i is the fractional anisotropy of the correlation time θ_i and r_∞ accounts for a nonzero background value at times $t \rightarrow \infty$. The initial anisotropy $r_0 = r(t{=}0)$ is given by

$$r_0 = r_\infty + r_1 + r_2 \qquad (7)$$

The goodness of all fits were determined by inspection of the weighted residuals and their autocorrelation functions as well as by inspection of the χ^2 values.

The alignment of the polarizers was tested by measuring the anisotropy of 2,5-diphenyloxazole (PPO, Merck) in ethylene glycol at 15 °C. A reconvolution analysis of the anisotropy decay (data not shown) resulted in an initial anisotropy of $r_0 = 0.337 \pm 0.004$ and a lifetime of $\tau = 1.516 \pm 0.003$ ns, which agrees well with the values published in ref 23.

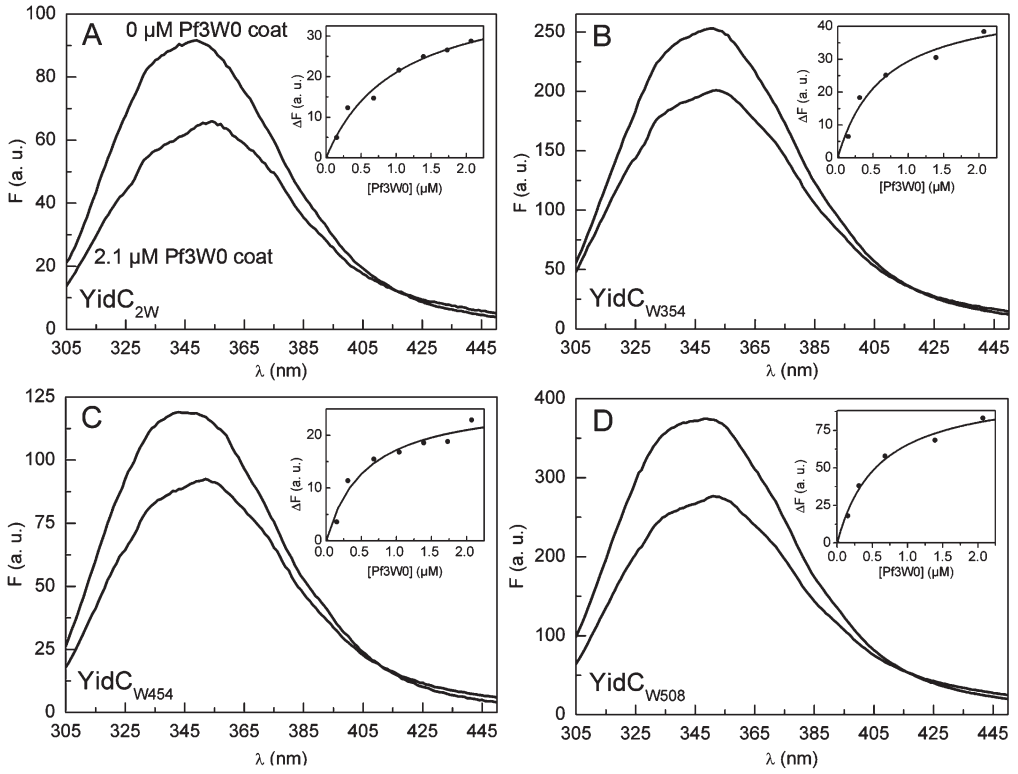

Figure 5. Instrinsic Trp fluorescence spectra of (A) $YidC_{2W}$, (B) $YidC_{W354}$, (C) $YidC_{W454}$, and (D) $YidC_{W508}$ (reconstituted in DOPC/DOPG vesicles) excited at 295 nm, before and after titration with Pf3W0 coat and, as shown in the insets, the corresponding binding curves constructed from the fluorescence values at 344 nm. The binding curves show best-fit K_D value of 0.97 ± 0.21 μM, 0.35 ± 0.09 μM, 0.83 ± 0.21 μM, and 0.76 ± 0.13 μM for $YidC_{2W}$, $YidC_{W354}$, $YidC_{W454}$, and $YidC_{W508}$, respectively [in 20 mM Tris-HCl (pH 7.0) and 300 mM NaCl and 5% (v/v) 2-propanol].

Fluorescence decay and anisotropy measurements of the reconstituted YidC mutants were done at a constant temperature of 25 °C prior and after the fluorometric titration experiment described above. Fluorescence decay of the P1 domain was measured in potassium phosphate buffer (PPB) at pH 6.0. All time-dependent measurements were analyzed with the FluoFit 4.4 software package (PicoQuant GmbH).

RESULTS

YidC Trp Mutants Are Fully Functional. To test the functionality of the His-tagged $YidC_{2W}$, $YidC_{W354}$, $YidC_{W454}$, and $YidC_{W508}$ as well as the His-tagged wild-type YidC, we analyzed whether these proteins complement the YidC depletion strain JS7131. In this strain, the genomic *yidC* gene is disrupted and a functional *yidC* gene is inserted at the *attB* locus. Additionally, the expression of the *yidC* gene is controlled by an *araBAD* promoter and operator. Hence, expression of chromosomal YidC is induced with arabinose but repressed with glucose. The *yidC* constructs are localized on the pGZ119EH vector and are controlled by a tac promoter so that expression of these constructs is induced by IPTG.

As a negative control, the empty vector pGZ119EH was tested. Complementation of the different YidC constructs was confirmed by restoring growth of strain JS7131 on LB agar plates containing glucose and IPTG (Figure 2). This proves that each plasmid-encoded, His-tagged YidC mutant as well as the His-tagged wild-type YidC is functional.

Membrane Topology of Reconstituted YidC Trp Mutants. The membrane topology of the reconstituted YidC mutants was examined by trypsin digestion of the proteoliposomes. If the proteins are reconstituted with the P1 domain inside the proteoliposomes ("loop-in" conformation), the proteolytic digestion generates a 42 kDa protected fragment[11] which contains the first and second transmembrane segment as well as the P1 domain. This fragment is detected by a P1-specific antiserum. If the mutants are reconstituted in the inverted direction, no such fragment is expected.

The results of the tryptic digest of the proteoliposomes are shown in Figure 3. For each mutant, the 42 kDa fragment was detected in significant amounts (lanes 2). Compared to the total amount of reconstituted protein (lanes 1), more than 60% of each mutant was found in the loop-in conformation. When the purified Trp mutants were solubilized exposing all the hydrophilic domains, no 42 kDa fragment was detected (lanes 3). These results show that for each mutant a large percentage (≈65%) of the protein was reconstituted with the P1 domain in the lumen of the DOPC/DOPG liposomes.

Binding of Pf3 Coat Protein to Liposomes. To evaluate whether the Pf3 coat protein binds to YidC as a soluble protein or from a membrane surface bound state, 21 μM of the protein was mixed with DOPC/DOPG liposomes. After centrifugation the amount of protein in the supernatant and in the pellet was analyzed. The analysis showed that about 50% of the protein was bound to the liposomes and 50% remained in the supernatant (Figure 3B). In conclusion, binding to YidC may occur from the soluble or from the membrane-bound Pf3 coat protein.

dx.doi.org/10.1021/bi1020293 |*Biochemistry* 2011, 50, 3229–3239

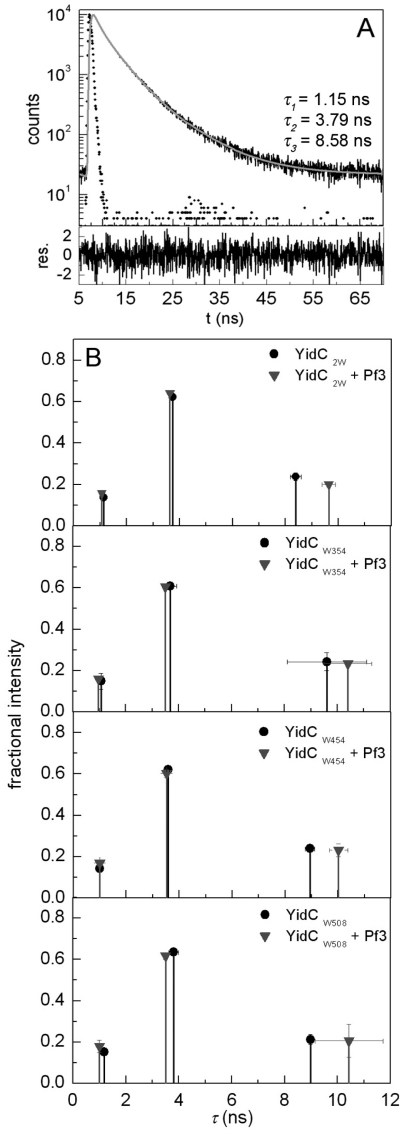

Figure 6. (A) Fluorescence decay of membrane-reconstituted $YidC_{2W}$ (full black line) excited at 290 nm with the fitted triple-exponential function (full gray line), and the instrument response function (dotted line) of the lifetime spectrometer. The weighted residuals (res.) for the triple-exponential fit are shown in the lower panel ($\chi^2 = 1.05$). (B) Mean values of the fluorescence decay components of reconstituted $YidC_{2W}$, $YidC_{W354}$, $YidC_{W454}$, and $YidC_{W508}$ before and after titration with Pf3W0 coat [in 20 mM Tris-HCl (pH 7.0) and 300 mM NaCl and 5% (v/v) 2-propanol].

Intrinsic Fluorescence Spectra of YidC Trp Mutants, YidCwt, and the P1 Loop. The proposed topology of YidC displayed in Figure 1A suggests that all Trp residues are located on the periplasmic side of the insertase. Steady-state fluorescence spectroscopy, at an excitation wavelength of 295 nm, was used to characterize the environments of the residues W332/W334 (2W), W354, W454, and W508. All single Trp mutants showed fluorescence spectra with similar characteristics. The best-fit values for the emission maxima λ_{max} are in the range of 344−346 nm, and the fwhm values are in the range of 66−69 nm. The double Trp mutant $YidC_{2W}$ exhibited a spectrum with a maximum at 345 nm and a fwhm of 67 nm, corresponding to the spectra obtained with the single Trp mutants. A fluorescence spectrum of $YidC_{2W}$, together with the log−normal fit (see eq 1), is shown in Figure 4A. A spectrum of membrane-reconstituted wild-type YidC is shown for comparison. Wild-type YidC exhibited a spectrum with a maximum at 346 nm and a fwhm of 64 nm. The measured λ_{max} values around 345 nm for the Trp mutants are indicative for a localization of those residues at the membrane/water interface of YidC.[24,25] In contrast, the fluorescence spectrum of the P1 domain (residues 56−329), whose three Trp residues are located in a compact and low-polar β-structure,[9,10] is blue-shifted to a λ_{max} of 334 nm and exhibited a considerably narrower spectrum with a fwhm of 57 nm.

In addition to its 11 Trp residues, the sequence of YidC includes 24 Tyr amino acid residues.[26] At excitation wavelengths in the range of 290 nm these 24 Tyr residues show an overall extinction which is similar to that of a single Trp residue, but Tyr emission is often quenched by carbonyl groups of the peptide backbone or neighboring residues.[27] Since the pulsed LED of the lifetime spectrometer emits at 290 nm (see Materials and Methods), the contribution of the Tyr residues to the fluorescence emission of an YidC single Trp mutant was examined. Spectra of reconstituted $YidC_{W508}$, excited at 290 and 295 nm, respectively, were recorded and compared after normalization to equal fluorescence yields at 420 nm. At which wavelength the fluorescence emission is due exclusively to Trp residues.[27] The normalized spectra and their difference spectrum are shown in Figure 4B. The difference spectrum indicates that there is an insignificant contribution of Tyr residues to the fluorescence of YidC when excited at 290 nm. In contrast, when excited at 280 nm line shape and spectral position of the difference spectrum show a distinct contribution of Tyr fluorescence to the emission spectrum as shown in Figure 4C. However, compared to the fluorescence of a single Trp residue, the 24 Tyr residues in the $YidC_{W508}$ molecule have a comparatively low quantum yield.

Fluorometric Titration of YidC Trp Mutants with Pf3W0 Coat. To test the binding behavior of the Trp mutants, samples containing 0.1 μM membrane-reconstituted YidC mutant protein were titrated with increasing amounts of Pf3W0 coat protein (0−2.1 μM). Figure 5 shows representative intrinsic fluorescence spectra excited at 295 nm for each mutant before and after titration with Pf3W0 coat. The corresponding binding curves constructed from the fluorescence data at 344 nm are shown in the insets. Fluorescence quenching upon titration with Pf3 coat was observed for all Trp mutants and is accompanied by a red shift and a spectral broadening of the emission. Red shift and broadening are both the range of 2−5 nm. All binding curves were fitted with sufficient accuracy to eq 2, and data analysis from two independent experiments yielded a mean dissociation constant K_D of 0.83 ± 0.15 μM for $YidC_{2W}$, 0.39 ± 0.05 μM for $YidC_{W354}$, 0.80 ± 0.1 μM for $YidC_{W454}$, and 0.87 ± 0.11 μM for $YidC_{W508}$. These data are consistent with the results from previous experiments with reconstituted wild-type YidC.[13]

Fluorescence Decay of YidC Trp Mutants before and after Binding to Pf3W0 Coat. Fluorescence decay measurements were performed at magic-angle conditions (54.7°) at an excitation wavelength of 290 nm with the same samples as used for the fluorometric titration experiments. The fluorescence decay of all single Trp mutants as well as the double Trp mutant, before and after binding, could be fitted with high accuracy with a triple-exponential function (see eq 3). A typical example of a fluorescence decay with the fitted triple-exponential function is shown in Figure 6A. The recovered liftetimes τ_i, given in this figure, and the corresponding fractional intensities (see eq 4) are

Table 1. Fluorescence Decay Parameters of YidC Mutants, P1 Domain (excited at 290 nm)[a]

	lifetime[b] (ns)			fractional amplitude[b]			average lifetime[c] (ns)
sample	τ_1	τ_2	τ_3	α_1	α_2	α_3	$\langle\tau\rangle$
YidC $_{2W}$	1.14 ± 0.01	3.74 ± 0.05	8.4 ± 0.2	0.38 ± 0.01	0.532 ± 0.004	0.091 ± 0.001	4.49 ± 0.03
YidC $_{2W}$ + Pf3W0 coat	1.06 ± 0.01	3.03 ± 0.02	9.6 ± 0.3	0.43 ± 0.01	0.51 ± 0.01	0.060 ± 0.002	4.42 ± 0.03
YidC $_{W354}$	1.1 ± 0.1	3.7 ± 0.2	9.6 ± 1.5	0.42 ± 0.04	0.50 ± 0.02	0.08 ± 0.03	4.7 ± 0.2
YidC $_{W354}$ + Pf3W0 coat	0.97 ± 0.02	3.50 ± 0.07	10.4 ± 0.9	0.46 ± 0.02	0.45 ± 0.02	0.06 ± 0.01	4.7 ± 0.1
YidC $_{W454}$	1.00 ± 0.05	3.59 ± 0.04	8.94 ± 0.18	0.41 ± 0.03	0.51 ± 0.02	0.080 ± 0.004	4.51 ± 0.01
YidC $_{W454}$ + Pf3W0 coat	1.00 ± 0.03	3.52 ± 0.09	10.0 ± 0.4	0.46 ± 0.01	0.480 ± 0.004	0.067 ± 0.01	4.6 ± 0.3
YidC$_{W508}$	1.2 ± 0.1	3.80 ± 0.2	8.98 ± 0.05	0.40 ± 0.01	0.522 ± 0.01	0.074 ± 0.007	4.50 ± 0.03
YidC $_{W508}$ + Pf3W0 coat	1.00 ± 0.04	3.50 ± 0.03	10.43 ± 0.01	0.47 ± 0.04	0.48 ± 0.03	0.06 ± 0.01	4.5 ± 0.1
YidC P1 loop (56 - 329)	4.28	6.56		0.96	0.04		4.41

[a] All errors are the standard deviations of the mean values. [b] Determined at magic angle (54.7°). [c] $\langle\tau\rangle = \Sigma\alpha_i\tau_i^2/\Sigma\alpha_i\tau_i$.

charcteristic for all investigated Trp mutants. Without substrate, all mutants have three distinct fluorescence lifetimes: $\tau_1 \approx 1$ ns, $\tau_2 \approx 4$ ns, and $\tau_3 \approx 9$ ns. After the addition of 2.1 μM Pf3 coat only τ_3 was extended by 1−2 ns concomitant with a decrease of its fractional amplitudes α_3, whereas τ_1 and τ_2, together with their α_i values, were not changed significantly. A graphical overview of the recovered lifetimes and their corresponding fractional intensities f_i (see eq 5) is shown in Figure 6B. The calculated lifetimes of all YidC Trp mutants, before and after binding to Pf3 coat, and their fractional amplitudes α_i are listed in Table 1. Two independent experiments were performed to obtain the standard deviations of the mean values.

In the preceding section it was mentioned that the three residues W252, W264, and W308 in the P1 domain (residues 56−329) are located in its low-polar β-supersandwich, resulting in a considerable red-shift of the intrinsic fluorescence. These three residues also differ in their lifetime data compared to the exposed residues in the Trp mutants. The fluorescence decay of P1 could be fitted with a double-exponential function (eq 3) revealing the lifetimes $\tau_1 = 4.28$ ns and $\tau_2 = 6.56$ ns, whereas the fractional amplitude of the shorter lifetime reaches nearly unity (Table 1).

Time-Resolved Fluorescence Anisotropy of YidC Trp Mutants before and after Binding to Pf3W0 Coat. Subsequent to the fluorescence decay measurements the vertical (I_{VV}) and horizontal (I_{VH}) decay component of the YidC sample were measured and the anisotropy $r(t)$ was calculated using eq 5. For all YidC Trp mutants, before and after binding, the calculated anisotropies could be fitted to a double-exponential function with a constant background value r_∞ (eq 6).

Without substrate, two correlation times with clearly distinct time scales were recovered: $\theta_1 \approx 1$ ns and $\theta_2 \approx 12$ ns for the mutants YidC$_{2W}$, YidC$_{W354}$, and YidC$_{W508}$ and $\theta_1 \approx 1$ ns and $\theta_2 \approx 17$ ns for YidC$_{W454}$. A typical example of the two fluorescence decay components and the calculated anisotropy with the fitted double-exponential function is shown in Figure 7A,B. After the addition of 2.1 μM Pf3 coat protein the shorter time θ_1 remained almost unchanged for all mutants, whereas the times θ_2 changed significantly. The largest change in the correlation times θ_2 is observed for the mutants YidC$_{2W}$ and YidC$_{W508}$, at which the times θ_2 almost double their values after binding to the substrate. The nonzero background value r_∞ is attributed to the rotation of the proteoliposomes. The rotational correlation times for a sphere with a diameter in the 100 nm range was calculated with the Stokes−Einstein equation (data not shown) and is in the order of magnitude of 100 μs.[22] Hence, the rotation of the proteoliposome is much too slow to contribute to an anisotropy decay on the nanosecond time scale. A graphical overview of the recovered correlation times and their corresponding fractional anisotropies is shown in Figure 7B. Two independent experiments were performed to obtain the standard deviations of the mean values except for YidC$_{W454}$ where only one significant measurement was obtained.

The initial anisotropy r_0 of Trp shows a strong dependence on the excitation wavelenght. For an excitation wavelength of 290 nm an initial anisotropy value of $r_0 = 0.13$ is expected.[28,29] The mean value of all recovered initial anisotropies (eq 7) was $r_0 = 0.11 \pm 0.01$ which is close to the literature value. This small deviation may indicate the existence of a subnanosecond relaxation processes, which cannot be resolved with our setup (IRF = 700 ps). The recovered correlation times of all YidC Trp mutants, before and after binding to Pf3 coat, their fractional anisotropies r_i and the r_0 values are summarized in Table 2.

DISCUSSION

For the insertion of a protein into the membrane the insertase YidC supports the translocation of the periplasmic domain across the membrane and the alignment of the hydrophobic regions of a substrate into the bilayer. These events are most likely due to major movements within YidC. In a previous study we have shown by steady-state Trp fluorescence spectroscopy that binding of Pf3 coat induces an overall conformational change of the YidC molecule.[13] The generation of three single Trp mutants and a double Trp mutant allowed us now to follow such changes in detail within the protein by steady-state and time-resolved methods. Since the single Trp residues were located in the P1, P2, and P3 loop, each of the periplasmic loops was followed separately. In parallel, all the mutants were tested in complementation assays with an YidC depletion strain of *E. coli* which proved the functionality of the YidC mutants.

Fluorimetric titration of the reconstituted YidC mutants with Pf3W0 coat was followed by quenching of the Trp residue(s) (Figure 5), indicating that the substrate-induced conformational change occurs in all three periplasmic loops of the insertase. The substrate binding constant for each of the mutants was determined, and all K_D values are in the range of $\approx$1 μM. This is in good agreement with the value for reconstituted wild-type YidC.[13] Furthermore, the nearly identical parameters of the intrinsic fluorescence profiles of all mutants (without substrate)

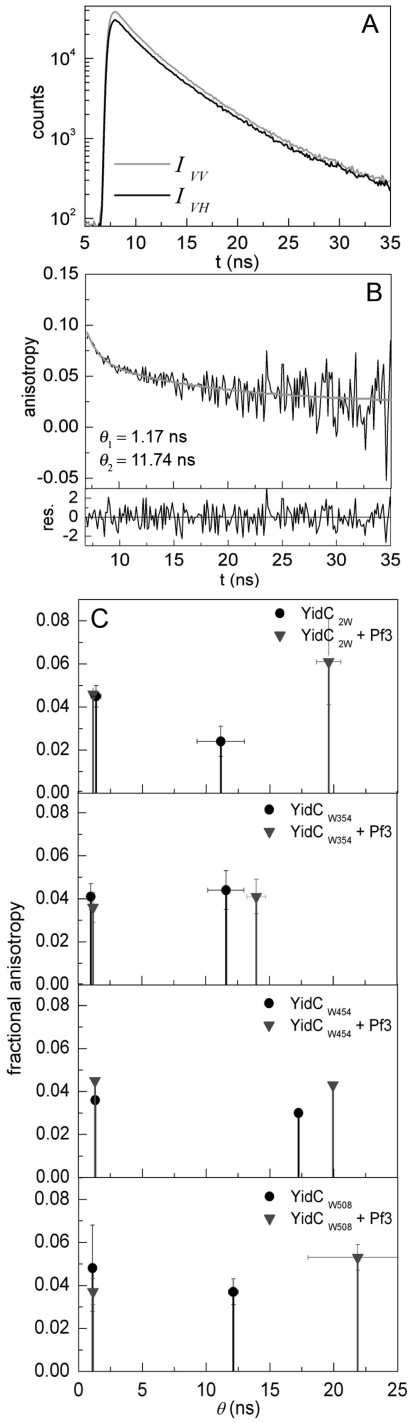

Figure 7. (A) Vertical (I_{VV}) and horizontal (I_{VH}) fluorescence decay components of membrane-reconstituted $YidC_{W508}$ excited at 290 nm with (B) the calculated anisotropy. The weighted residuals (res.) for the double-exponential fit (full gray line) are shown in the lower panel (χ^2 = 1.0). (C) Mean values of the anisotropy components of $YidC_{2W}$, $YidC_{W354}$, $YidC_{W454}$, and $YidC_{W508}$ before and after titration with Pf3W0 coat [in 20 mM Tris-HCl (pH 7.0) and 300 mM NaCl and 5% (v/v) 2-propanol].

reveal that their Trp residues are located in similar environments. The measured fluorescence maxima $\lambda_{max} \approx 345$ nm are charcteristic for Trp residues in an amphiphilic environment.[24,25]

According to the proposed membrane topology in Figure 1A, the Trp residues W354, W454, and W508 are located at the membrane/water interface. This proposed location of Trp residues is consistent with our results.

All Trp residues in the large periplasmic domain P1 were resolved in the crystal structure reported by Oliver and Paetzel[9] which is shown in Figure 1B. The structure reveals that the W252, W264, and W308 are located in the compact and low-polar β-structure of P1 with a low accessibility for water molecules. In contrast, the residues at W332 and W334 are located at a short α-helical segment with their indole moieties both partially exposed to the polar aqueous surrounding. The different environments of these residues are compatible with the fluorescence spectra of our P1 sample (with the residues W252, W264, and W308) and $YidC_{2W}$ (residues W332 and W334) shown in Figure 4. Whereas the intrinsic fluorescence spectrum of $YidC_{2W}$ has its maximum at λ_{max} = 345 nm, the spectrum of the P1 loop was considerably blue-shifted by 11 nm, which is indicative for a low-polar environment of the Trp residues W252, W264, and W308.[24,25]

Fluorescence decays of all YidC mutants, before and after binding to PfW0 coat, were fitted with a triple-exponential model, and lifetimes with distinct time scales ($\tau_1 \approx 1$ ns, $\tau_2 \approx 4$ ns, and $\tau_3 \approx 9$ ns) were recovered. Because of the limited time resolution of the setup (IRF = 700 ps), the existence of further unresolved components in the subnanosecond range cannot be excluded. However, our results are in good agreement with the multiexponential decay data reported for a number of other single- and double-Trp-containing proteins.[27,30] Although the interpretation of the decay times is complicated, triple-exponential decays are often analyzed using the rotamer model.[31] Other studies indicate that chemical heterogeneity as well as relaxation processes of the indole environment are responsible for multi-exponential fluorescence behavior of Trp residues.[25,32] Furthermore, in large proteins interactions of the Trp residue with the peptide backbone and with neighboring residues have to be considered. Consequently, we will interpret the decay data in more general terms as a result of the changed environment of the Trp residues. The similar lifetimes for all mutants without Pf3W0 coat suggest that the Trp residues W332/W334, W354, W454, and W508 are present in equivalent environments. These environments seem to change uniformly upon binding because all mutants showed a significant extended τ_3 value after the addition of Pf3W0 coat, whereas only minor changes were observed for the other lifetime components (Table 1 and Figure 6). These findings are supported by the similarity of the intrinsic fluorescence spectra of the Trp mutants before and after binding to Pf3W0 coat (Figure 5). The constancy of the average lifetimes (Table 1), before and after binding of YidC to the coat protein, indicates that the substrate-induced fluorescence quenching is governed by a static process. The extent of the quenching at substrate saturation concentration can be estimated from the binding curves (Figure 5) and the results from the topology analysis (Figure 3). Analysis of the binding curves shows that for each mutant the quenching at saturation does not exceed 56% of the initial fluorescence (data not shown). From this together with the result that more than 60% of each mutant is reconstituted in the loop-in conformation, we conclude that around 80% of the Trp fluorescence will be quenched when YidC is saturated with Pf3coat. This extent of quenching is comparable to results found in other protein−substrate or protein−lipid interaction studies.[33,34]

Table 2. Fluorescence Anisotropy Decay Parameters of YidC Mutants (excited at 290 nm)[a]

	correlation time (ns)		fractional anisotropy		initial anisotropy[b]
sample	θ_1	θ_2	r_1	r_2	r_0
YidC $_{2W}$	1.4 ± 0.4	11.1 ± 1.9	0.045 ± 0.005	0.024 ± 0.007	0.11 ± 0.01
YidC $_{2W}$ + Pf3W0 coat	1.13 ± 0.01	19.6 ± 0.9	0.046 ± 0.001	0.06 ± 0.02	0.12 ± 0.02
YidC $_{W354}$	1.00 ± 0.03	11.6 ± 1.4	0.041 ± 0.006	0.044 ± 0.009	0.11 ± 0.01
YidC $_{W354}$ + Pf3W0 coat	1.17 ± 0.03	14.0 ± 0.7	0.036 ± 0.007	0.041 ± 0.008	0.11 ± 0.01
YidC $_{W454}$	1.32	17.25	0.036	0.030	0.11
YidC $_{W454}$ + Pf3W0 coat	1.3	19.94	0.045	0.043	0.10
YidC$_{W508}$	1.08 ± 0.09	12.1 ± 0.4	0.05 ± 0.02	0.037 ± 0.006	0.11 ± 0.03
YidC $_{W508}$ + Pf3W0 coat	1.12 ± 0.08	21.9 ± 3.8	0.041 ± 0.005	0.053 ± 0.006	0.12 ± 0.01

[a] All errors are the standard deviations of the mean values. [b] $r_0 = r_\infty + r_1 + r_2$.

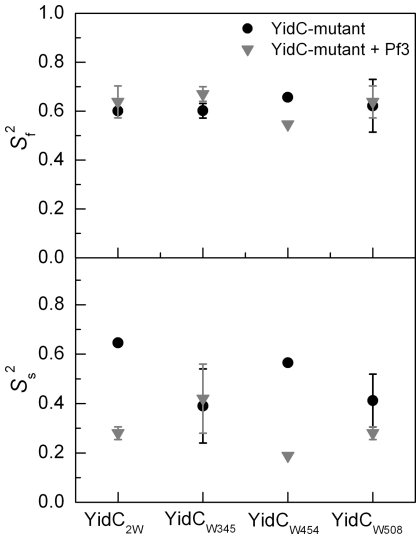

Figure 8. Order parameters S_f^2 (upper panel) and S_s^2 (lower panel) of the different YidC Trp mutants before and after binding of Pf3W0 coat protein. The error bars show the standard deviations of the mean values.

The binding of the Pf3 coat protein to YidC could occur directly from the aqueous environment or after a partial partition of the Pf3 coat protein into the cytoplasmic leaflet of the membrane and a subsequent lateral binding to YidC. Since the Pf3 protein was equally present in the membrane and in the soluble in the absence of YidC (Figure 3B) we cannot distinguish between the two possibilities.

The low-polar environment inside the β-structure of the P1 domain (Figure 1B) considerably affects the fluorescence decay behavior of the Trp residues at positions 252, 264, and 308. Instead of a complex triple-exponential decay, a nearly single-exponential decay was observed for these three residues (Table 1). We conclude that the lifetime data for our YidC mutants as well as for the P1 domain are consistent with the findings from the steady-state spectroscopy and with the supposed membrane topology of YidC.

Fluorescence anisotropy of all Trp mutants was analyzed with a simple double-exponential model including a nonzero background value which accounts for the overall motion of YidC embedded in membrane vesicles (see Results). Thus, the recovered correlation times θ_1 and θ_2 indicate the existence of an internal flexibility of the Trp residues. Such a flexibility arises from internal motions, of the indole moiety, e.g., by oscillations and rotation as well as from wobbling motions of the entire Trp residue due to the flexibility of the peptide backbone. NMR studies of protein dynamics revealed that the correlation times for backbone motions can vary over several orders of magnitude from 10 ns for large segmental motions of protein domains[35,36] down to 50 ps for highly restricted motions.[37] Short time dynamics in the picosecond range were predicted by theoretical studies[38] which attribute this fast processes to librational motions of the indole moiety about its $C_\alpha - C_\beta$ and $C_\beta - C_\gamma$ bonds. In addition, solid-state NMR experiments with bacteriorhodopsin revealed that aromatic residues undergo 2-site jumps with correlation times in the range of ≤10 ns.[39,40] However, correlation times around 1 ns are usually attributed to restricted motions of the Trp residue. The appearance of a second correlation time θ_2, belonging to internal motions of Trp residues, with $\theta_2 \approx 10$ ns is seldomly reported from fluorescence anisotropy experiments,[41−43] but NMR data from other proteins indicate that backbone motions can occur on a nanoseconds time scale.[35,36] Drawing an analogy to the NMR data, we therefore attribute the correlation time θ_2 to motions of the Trp residues relating to the backbone mobility. The existence of a third unresolved decay component ($\theta_3 \ll 1$ ns) is suggested by the difference between the expected initial anisotropy of $r_0 = 0.13$ and the experimentally recovered value of $r_0 = 0.11 \pm 0.01$ (mean from all experiments).

In the case of two correlation times which differ by at least 1 order of magnitude, the motion of the Trp residues can be analyzed with[44,45]

$$C(t) = r(t)/r_0 = S_f^2 S_s^2 + (1 - S_f^2)\exp(-t/\theta_1) + S_f^2(1 - S_s^2)\exp(-t/\theta_2)$$

with order parameters S_f^2 and S_s^2 which characterize the fast and the slow fluctuations, respectively. $S_{f,s}^2$ are given by $S_f^2 = (r_2 + r_\infty)/r_0$ and $S_s^2 = r_\infty/(r_2 + r_\infty)$. The results of this analysis are summarized in Figure 8. The parameter S_f^2 (Figure 8, upper panel), corresponding to the short correlation time θ_1, shows a fairly constant value of ≈0.6, indicating a restricted motion of the residue(s) which is not influenced by the binding process. In contrast, S_s^2 (Figure 8, lower panel), corresponding to the correlation time θ_2, shows a dependency on binding of Pf3 coat as well as on on the position of the Trp residue(s) along the periplasmic loops. The S_s^2 values for YidC$_{2W}$, YidC$_{W454}$, and YidC$_{W508}$ are significantly lower when the Pf3 coat protein is bound to the insertase. indicating a higher mobility of the corresponding backbone segment. In particular, for the residues

W332/W334 (2W) and W508 these changes in mobility are concomitant with an explicit increase of the corresponding correlation time. Similar behavior upon ligand binding, i.e., an increase of segmental mobilty, was reported in other protein−ligand interaction studies using time-resolved Trp fluorescence anisotropy.[46,47]

In vivo cross-linking experiments had proven that Pf3 coat protein comes into close contact with the YidC domains TM1 and TM3.[48] We assume that this interaction of Pf3 coat with TM1 is responsible for the measured change in the mobility of the residues W332/334 in the P1 backbone which is directly connected to TM1 (see Figure 1).

Taken together, our results from steady-state and time-resolved fluorescence spectroscopy are consistent with the proposed membrane topology of YidC and the structure of the P1 periplasmic domain. Fluorimetric titration of the YidC Trp mutants revealed that the substrate-induced conformational change affects all periplasmic domains P1, P2, and P3. Furthermore, our fluorescence anisotropy data showed that this substrate-induced change within YidC affects individual motions within all periplasmic transmembrane regions of the insertase, whereas the large periplasmic domain P1 retains its folded structure but shows considerable backbone movement relative to the membrane moiety of YidC.

AUTHOR INFORMATION

Corresponding Author

*Tel: ++49-711-459 23885. Fax: ++49-711-459 22238. E-mail: gerken@uni-hohenheim.de.

Funding Sources

This work was supported by the DFG grant KU749/6-1.

ACKNOWLEDGMENT

We thank Dr. Robin Ghosh for fruitful discussions and the review of the manuscript and PicoQuant GmbH for their support to the time-resolved spectroscopy experiments. We also thank Benno Lissy and Reinhold Renner from the mechanical workshop for the fast and uncomplicated fabrication of the rotatable polarizer mount.

ABBREVIATIONS

DDM, *n*-dodecyl-β-D-maltoside; DOPC, 1,2-dioleoyl-*sn*-glycero-3-phosphocholine; DOPG, 1,2-dioleoyl-*sn*-glycero-3-phospho-(1′-*rac*-glycerol); ECL, enhanced chemoluminescence; fwhm, full width at half-maximum; IPTG, isopropyl-β-D-thiogalactopyranoside; IRF, instrument response function; NTA, nitrilotriacetic acid; PPB, potassium phosphate buffer; SDS, sodium dodecyl sulfate; TCA, trichloroacetic acid; TBS, Tris-buffered saline; TCSPC, time-correlated single photon counting; Tris, 2-amino-2-(hydroxymethyl)-1,3-propanediol.

REFERENCES

(1) Rapoport, T. A. (2007) Protein translocation across the eukaryotic endoplasmic reticulum and the bacterial plasma membranes. *Nature 450*, 663–669.

(2) Van den Berg, B., Clemons, W. M., Collinson, I., Modis, Y., Hartmann, E., Harrison, S. C., and Rapoport, T. A. (2004) X-ray structure of a protein-conducting channel. *Nature 427*, 36–44.

(3) Xie, K., Hessa, T., Seppalä, S., Rapp, M., von Heijne, G., and Dalbey, R. E. (2007) Features of transmembrane segments that promote the lateral release from the translocase into the lipid phase. *Biochemistry 46*, 15153–15161.

(4) Samuelson, J. C., Chen, M., Jiang, F., Möller, I., Wiedmann, M., Kuhn, A., Phillips, G. J., and Dalbey, R. E. (2000) YidC mediates membrane protein insertion in bacteria. *Nature 406*, 637–641.

(5) Kuhn, A. (1995) Bacteriophage Pf3 and M13 as model systems for Sec-independent protein transport. *FEMS Microbiol. Rev. 17*, 185–190.

(6) van der Laan, M., Bechtluft, P., Kol, S., Nouwen, N., and Driessen, A. J. (2004) F_1F_o ATP synthase subunit c is a substrate of the novel YidC pathway for membrane protein biogenesis. *J. Cell Biol. 165*, 213–222.

(7) Facey, S. J., Neugebauer, S. A., Krauss, S., and Kuhn, A. (2007) The mechanosensitive channel protein MscL is targeted by the SRP to the novel YidC membrane insertion pathway of *Escherichia coli*. *J. Mol. Biol. 365*, 995–1004.

(8) Sääf, A., Monne, M., de Gier, J. W. L., and von Heijne, G. (1998) Membrane Topology of the 60-kDa Oxa1p Homologue from *Escherichia coli*. *J. Biol. Chem. 273*, 30415–30418.

(9) Oliver, D. C., and Paetzel, M. (2008) Crystal structure of the major periplasmic domain of the bacterial membrane protein assembly facilitator YidC. *J. Biol. Chem. 283*, 5208–5216.

(10) Ravaud, S., Stjepanovic, G., Wild, K., and Sinning, I. (2008) The crystal structure of the periplasmic domain of the *Escherichia coli* membrane protein insertase YidC contains a substrate binding cleft. *J. Biol. Chem. 283*, 9350–9358.

(11) Serek, J., Bauer-Manz, G., Struhalla, G., van den Berg, L., Kiefer, D., Dalbey, R. E., and Kuhn, A. (2004) *Escherichia coli* YidC is a membrane insertase for Sec-independent proteins. *EMBO J. 23*, 295–301.

(12) Gerken, U., Erhardt, D., Bär, G., Ghosh, R., and Kuhn, A. (2008) Initial binding process of the membrane insertase YidC with its substrate Pf3 coat protein is reversible. *Biochemistry 47*, 6052–6058.

(13) Winterfeld, S., Imhof, N., Roos, T., Bär, G., Kuhn, A., and Gerken, U. (2009) Substrate-induced conformational change of the *Escherichia coli* membrane insertase YidC. *Biochemistry 48*, 6684–6691.

(14) Yanisch-Perron, C., Vieira, J., and Messing, J. (1985) Improved M13 phage cloning vectors and host strains: nucleotide sequences of the M13mpl8 and pUC19 vectors. *Gene 33*, 103–119.

(15) Kiefer, D., and Kuhn, A. (1999) Hydrophobic forces drive spontaneous membrane insertion of the bacteriophage Pf3 coat protein without topological control. *EMBO J. 18*, 6299–6306.

(16) Lessl, M., Balzer, D., Lurz, R., Waters, V. L., Guiney, D. G., and Lanka, E. (1992) Dissection of IncP conjugative plasmid transfer: Definition of the transfer region Tra2 by mobilization of the Tra1 region in *trans*. *J. Bacteriol. 174*, 2493–2500.

(17) Lowry, O. H., Rosebrough, N. J., Farr, A. L., and Randall, R. J. (1951) Protein measurement with Foline phenol reagent. *J. Biol. Chem. 193*, 265–275.

(18) Rigaud, J. L., Paternostre, M. T., and Bluzat, A. (1988) Mechanisms of membrane protein insertion into liposomes during reconstitution procedures involving the use of detergents. 2. Incorporation of the light-driven proton pump bacteriorhodopsin. *Biochemistry 27*, 2677–2688.

(19) Balzer, D., Ziegelin, G., Pansegrau, W., Kruft, V., and Lanka, E. (1992) KorB protein of promiscuous plasmid RP4 recognizes inverted sequence repetitions in regions essential for conjugative plasmid transfer. *Nucleic Acids Res. 20*, 1851–1858.

(20) Ladokhin, A. S., Jayasinghe, S., and White, A. (2000) How to measure and analyze tryptophan fluorescence in membranes properly, and why bother? *Anal Biochem. 285*, 235–245.

(21) Ladokhin, A. S., and Holloway, P. W. (1995) Fluorescence of membrane-bound tryptophan octyl ester: Studying intrinsic fluorescence of protein-membrane interactions. *Biophys. J. 69*, 506–517.

(22) Gerken, U., and Imhof, N. (2010) PicoQuant Application Note: Time-resolved spectroscopy of proteins. http://www.picoquant.com/appnotes.htm.

(23) Lakowicz, J. R., Gryczsynski, I., Gryczsynski, Z., Danielsen, E., and Wirth, M. J. (1992) Time-resolved fluorescence intensity and anisotropy decays of 2,5-diphenyloxazole by two-photon excitation and frequency-domain fluorometry. *J. Phys. Chem. 96*, 3000–3006.

(24) Vivian, J. T., and Callis, R. C. (2001) Mechanism of tryptophan fluorescence shifts in proteins. *Biophys. J. 80*, 2093–2109.

(25) Burstein, E. A., Vedenkina, N. S., and Ivkova, M. N. (1973) Fluorescence and the location of tryptophan residues in protein molecules. *Photochem. Photobiol. 18*, 263–279.

(26) Kiefer, D., and Kuhn, A. (2007) YidC as an essential and multifunctional component in membrane protein assembly. *Int. Rev. Cytol. 259*, 113–138.

(27) Lakowicz, J. R. (1999) *Principles of Fluorescence Spectroscopy*, 2nd ed., Kluwer Academics/Plenum Publisher, New York.

(28) Valeur, B., and Weber, G. (1977) Resolution of the excitation spectrum of indole into the ^1L_a and ^1L_b excitation bands. *Photochem. Photobiol. 25*, 441–444.

(29) Ruggiero, A. J., Todd, D. C., and Fleming, G.. R. (1990) Subpicosecond fluorescence anisotropy of tryptophan in water. *J. Am. Chem. Soc. 112*, 1003–1014.

(30) Beecham, J. M., and Brand, L. (1985) Time-resolved fluorescence of proteins. *Annu. Rev. Biochem. 54*, 43–71.

(31) Szabo, A. G., and Rayner, D. M. (1980) Fluorescence decay of tryptophan conformers in solution. *J. Am. Chem. Soc. 102*, 554–563.

(32) Gakamsky, D. M., Demchenko, A. P., Nemkovich, N. A., Rubinov, A. N., Tomin, V. I., and Shcherbatska, N. V. (1992) Selective laser spectroscopy of 1-phenylnaphthylamine in phospholipid membranes. *Biophys. Chem. 42*, 49–61.

(33) Jang, D.-J., and El-Sayed, M. A. (1989) Tryptophan fluorescence quenching as a monitor for the protein conformation changes occuring during the photocycle of bacteriorhodopsin under different perturbations. *Proc. Natl. Acad. Sci. U.S.A. 86*, 5815–5819.

(34) Macheroux, P., Schönbrunn, E., Svergun, D. I., Volkov, V. V., Koch, M. H., Bornemann, S., and Thorneley, R. N. (1998) Evidence for a major structural change in *Escherichia coli* chorismate synthase induced by flavin and substrate binding. *Biochem. J. 335*, 319–327.

(35) Alexandrescu, A. T., and Shortle, D. (1994) Backbone dynamics of a highly restricted disordered 131 residue fragment of staphylococcal nuclease. *J. Mol. Biol. 242*, 527–546.

(36) Chevelkov, V., Fink, U., and Reiff, B. (2009) Quantitative analysis of the backbone motion in proteins using MAS solid-state NMR spectroscopy. *J. Biomol. NMR 45*, 197–206.

(37) Chen, C., Feng, Y., Short, J. H., and Wand, A. J. (1993) The main chain dynamics of a peptide bound to calmodulin. *Arch. Biochem. Biophys. 306*, 510–514.

(38) Ichiye, T., and Karplus, M. (1983) Fluorescence depolarization of tryptophan residues in proteins: A molecular dynamics study. *Biochemistry 22*, 2884–2893.

(39) Rice, D. M., Blume, A., Herzfeld, J., Wittebort, R. J., Huang, T.-H., Das Gupta, S. K., and Griffin, R. G. (1981) Solid State NMR Investigations of Lipid Bilayers, Peptides, and Proteins. *Biomolecular Stereodynamics*, Vol. 2, pp 255−270, Adenine Press, New York.

(40) Wüthrich, K. (1995) *NMR in Structural Biology*, World Scientific Publishing Co. Pte. Ltd., Singapore.

(41) Johnson, I. D., and Hudson, B. (1988) Environmental modulation of M13 coat protein tryptophan fluorescence dynamics. *Biochemistry 28*, 6392–6400.

(42) Datema, K. P., Visser, A. J. W. G., van Hoek, A., Wolfs, C. J. A. M., Spruijt, R. B., and Hemminga, W. A. (1987) Time−resolved tryptophan fluorescence anisotropy investigation of bacteriophage M13 coat protein in micelles an mixed bilayers. *Biochemistry 26*, 6145–6152.

(43) Vogel, H., Nilsson, L., Rigler, R., Voges, K. P., and Jung, G. (1988) Structural fluctuations of a helical polypeptide traversing a lipid bilayer. *Proc. Natl. Acad. Sci. U.S.A. 85*, 5067–5071.

(44) Clore, G. M., Driscoll, P. C., Wingfield, P. T., and Gronenborn, A. M. (1990) Analysis of the backbone dynamics of interleukin-1 β using two-dimensional inverse detected heteronuclear ^{15}N-^{1}H NMR spectroscopy. *Biochemistry 29*, 7387–7401.

(45) Silvi Antonini, P., Hillen, W., Ettner, N., Hinrichs, W., Fantucci, P., Doglia, S. M., Bousquet, J. A., and Chabbert, M. (1997) Molecular mechanics analysis of Tet repressor TRP-43 fluorescence. *Biophys. J. 72*, 1800–1811.

(46) Karkaria, C. E., Steiner, R. F., and Rosen, B. P. (1991) Ligand interactions in the ArsA protein, the catalytic component of an anion-translocating adenosinetriphosphatase. *Biochemistry 30*, 2635–2638.

(47) Sopkova, J., Gallay, J., Vincent, M., Pancoska, P., and Lewit-Bentley, A. (1994) The dynamic behavior of annexin V as a function of calcium ion binding: a circular dichroism, UV absorption, and steady-state and time-resolved fluorescence study. *Biochemistry 33*, 4490–4499.

(48) Klenner, C., Yuan, J., Dalbey, R. E., and Kuhn, A. (2008) The Pf3 coat protein contacts TM1 and TM3 of YidC during membrane biogenesis. *FEBS Lett. 582*, 3967–3972.